to an increase in $N_0(E_F)$. However, K is relatively constant between 2 and 6%.

CONCLUSIONS

The variation of the electronic specific heat γ with concentration does not follow that of the isotropic Knight shift. γ shows no dip but rather a rapid rise which may possibly be due to the contribution of third-zone α arms to the density of states.

ACKNOWLEDGMENT

The authors wish to acknowledge the assistance of Mark Bierschback in analyzing the data.

PHYSICAL REVIEW B VOLUME 1, NUMBER 2 15 JANUARY 1970

Magnetoacoustic Measurements of the Fermi Surface of Copper

G. N. KAMM
Naval Research Laboratory, Washington, D. C. 20390
(Received 11 September 1969)

Oscillations in the attenuation of 600-MHz LA waves propagated along the principal symmetry direction of copper single crystals are examined as a function of magnetic field in a perpendicular plane. Frequencies of the magnetoacoustic oscillations are associated with the responsible electron-orbit groups on the Fermi surface and, from them, radial dimensions are derived. These dimensions are standardized by means of open-orbit resonances in terms of Brillouin-zone dimensions. This also gives an independent measurement of the velocity of sound at ultrahigh frequencies. A close correlation is found between measured dimensions and the Koringa-Kohn-Rostoker (KKR) calculation by Faulkner *et al.* A generally good fit of the measured dimensions to a recent synthesis of the copper Fermi surface by Halse and Shoenberg from de Haas–van Alphen (dHvA) data is also observed.

I. INTRODUCTION

THE attenuation of sound in pure metals at low temperatures is dominated by an electronic contribution. When the mean free path of the electrons is long compared to the wavelength, magnetoacoustic oscillations (transverse-field dimensional resonances) in the ultrasonic attenuation are observed when an applied magnetic field is varied. Such studies, performed on high-purity single crystals, can allow a projection of the Fermi surface on a plane perpendicular to the sound-wave direction to be directly delineated. Very adequate surveys of magnetoacoustic methods together with extensive references are available, e.g., by Tepley,[1] Gavenda,[2] Peverley,[3] and Roberts.[4] A semiclassical theoretical treatment of magnetoacoustic oscillations applicable to the present experimental conditions has been given for a spherical Fermi-surface model by Cohen, Harrison, and Harrison.[5] A comparable treatment of a cylindrical Fermi-surface model which incorporated open orbits and possibility of magnetic breakdown has been given by Sievert.[6]

An important application of accurate Fermi-surface dimensions obtained by the magnetoacoustic method is the evaluation of the assumptions made in band-structure calculations. The recent self-consistent augmented-plane-wave (APW) calculations for copper by Snow and Waber[7] and the Koringa-Kohn-Rostoker (KKR) calculations by Faulkner, Davis, and Joy[8] have made an accurate experimental study of copper appropriate. The direct Fermi radii such as are given by the magnetoacoustic method are best suited for this purpose. More accurate magnetoacoustic measurements are now possible because copper crystals having a long electron mean free path can be prepared and because the form of the Fermi surface is sufficiently simple that the identification of the many oscillation frequencies with electron orbits can be made unambiguously.

The magnetoacoustic effect supplements other methods of Fermi-surface study such as galvanomagnetic measurements, rf size effect, cyclotron resonance studies, and quantum oscillation effects. The basic requirement on specimen purity is that $ql \gg 1$. The quantity l is the electron mean free path and q is the magnitude of the sound-propagation vector, given by $2\pi/\lambda$, where λ is the sound wavelength. This is generally more severe than

[1] N. Tepley, Proc. IEEE **53**, 1586 (1965).
[2] J. D. Gavenda, in *Progress in Applied Materials Research* (Gordon and Breach, Science Publishers, Inc., New York, 1964), Vol. VI, p. 43.
[3] J. R. Peverley, in *Physical Acoustics*, edited by W. P. Mason (Academic Press Inc., New York, 1966), Vol. IV, Part A, Chap. 9, p. 353.
[4] B. W. Roberts, in *Physical Acoustics*, edited by W. P. Mason (Academic Press Inc., New York, 1968), Vol. IV, Part B, Chap. 10, p. 1.
[5] M. H. Cohen, M. J. Harrison, and W. A. Harrison, Phys. Rev. **117**, 937 (1960).
[6] P. R. Sievert, Phys. Rev. **161**, 637 (1967).
[7] E. C. Snow and J. T. Waber, Phys. Rev. **157**, 570 (1967).
[8] J. W. Faulkner, H. L. Davis, and H. W. Joy, Phys. Rev. **161**, 656 (1967).

for de Haas–van Alphen (dHvA) effect measurements but less so than for rf size effect and cyclotron resonance work, which require that the product of angular frequency and relaxation time exceed and preferably be much larger than one. Although a magnetoacoustic specimen is required to have a surface flat and parallel within a wavelength of sound, there is no need for an atomically perfect surface within the electromagnetic skin depth.

Radial Fermi-surface dimensions can, of course, also be determined from dHvA measurements of extremal areas by fitting these extremal areas to an analytic expression for the Fermi surface. For copper, a Fourier expansion synthesis was made by Roaf[9] from measurements of Shoenberg,[10] and, more recently, by Halse[11] from measurements of Joseph *et al.*[12] An expansion in cubic harmonics has been made by Zornberg and Mueller.[13] In Sec. IV and in Table IV, the magnetoacoustic results are compared with these radii and with the results of band-structure calculations.

For a cubic crystal, only three crystallographic directions allow the propagation of a pure longitudinal (or shear) mode; the ⟨100⟩, ⟨110⟩, and ⟨111⟩ directions. These directions were chosen for the propagation of longitudinal-mode waves in order to avoid any possibility of ambiguity in interpretation arising from mode conversion, and also to simplify the interpretation, since extremal dimensions, measured in symmetry planes, are more easily related to the desired radial dimensions. Limited measurements were made, however, with a ⟨112⟩ sound direction. Similar longitudinal-wave magnetoacoustic studies on copper have been made by Morse, Meyer, and Walker,[14] by Bohm and Easterling,[15] and by Peverley.[3] In this paper, a considerably more complete description of the oscillations is given, and, for the first time, the dimensional data has been related to the Brillouin zone by use of open orbits.

When the magnetic field **B** is transverse to the sound-wave vector **q**, the form of the electron path in real space matches a cross section of the Fermi surface perpendicular to **B** but scaled and rotated by 90°. The measured dimension on the Fermi surface is, thus, perpendicular to both **B** and **q** and is given by $\Delta k = 2k = e\lambda F/ch$, where F is oscillation frequency in gauss (the reciprocal of the period in $1/B$), λ is the wavelength of sound, and hk is the momentum, k being considered a radial dimension, and Δk is the spacing between extremal regions. The extremal or "caliper" dimensions are those for which Δk is essentially unchanged for adjacent orbits on the Fermi surface displaced in the direction of **B**.

Open orbits are possible in copper because of the existence of necks on the Fermi surface. Open-orbit resonances are possible when the open orbit is periodic and has a component in real space in the direction of **q**. While magnetoacoustic oscillations exhibit, in general, a phase factor, in the case of open-orbit resonances the phase is zero, since all of the contributing electrons have the same periodicity in the direction of the sound wave, dictated by the Brillouin-zone spacing. Because their numbers are relatively small and their interaction with the sound wave is low, such electrons make relatively little contribution to the general attenuation pattern except at resonances. The oscillations are already prominent for $ql=10$; however, the open-orbit effect is negligible. Open-orbit resonances are accentuated when the mean free path is long. In these experiments, where ql is in the range 150–600, the number of magnetoacoustic oscillations is large enough to yield good precision. The open-orbit resonances are sharp and offer the alternative of standardizing dimensions relative to the Brillouin-zone spacing independently of knowing the sound wavelength λ through the velocity of sound. For convenience in presentation, and because the Brillouin-zone spacings are to be the reference standards used in interpreting dimensions, Fermi-surface dimensions will be given in dimensionless units of ka, where a is the cubic lattice constant.

II. EXPERIMENTAL PROCEDURE

Longitudinal ultrasonic waves with a frequency of about 600 MHz have been used in a study of magnetoacoustic oscillations in copper. In these experiments, the magnetic field is perpendicular to the sound wave and ranges from 0 to 25 kG. All measurements were performed at a temperature of 4.2°K. The specimen assembly and ultrasonic system employed in these measurements are essentially as described by Kamm and Bohm.[16] A conventional pulse-echo technique was used with X-cut quartz transducers having a 20-MHz fundamental resonance but driven at a high (odd) harmonic. Since the pulse delay through the specimen, typically about 0.15 cm thick, was small, a Z-cut quartz delay rod 2.5 cm long was introduced to allow receiver recovery to be complete. A pulse length of 2 μsec was chosen for the measurements, short enough to achieve a good separation of the delayed signal from the transmitter pulse but long enough, with over 1000 oscillations, to give a good definition of the ultrasonic frequency. The frequency was measured with a crystal-calibrated rf signal generator. The pulse modulator waveform was carefully shaped to minimize frequency

[9] D. J. Roaf, Phil. Trans. Roy. Soc. London **255A**, 135 (1962).
[10] D. Shoenberg, Trans. Roy. Soc. Can. **255A**, 85 (1962).
[11] M. Halse, Ph.D. thesis, Cambridge University, 1967 (unpublished).
[12] A. S. Joseph, A. C. Thornsen, E. Gertner, and L. E. Valby, Phys. Rev. **148**, 569 (1966).
[13] E. I. Zornberg and F. M. Mueller, Phys. Rev. **151**, 557 (1966).
[14] R. W. Morse, A. Myers, and C. T. Walker, J. Acoust. Soc. Am. **33**, 699 (1961).
[15] H. V. Bohm and V. J. Easterling, Phys. Rev. **128**, 1021 (1962).
[16] G. N. Kamm and H. V. Bohm, Rev. Sci. Instr. **33**, 957 (1962).

modulation during the pulse. The ultrasonic signal was recorded as a function of the inverse of magnetic field to facilitate the identification of the characteristic frequencies. Some of the data were taken in an air core (Helmholtz pair) magnet for which magnet current was an accurate measure of the field. Most of the measurements, however, were made in a conventional iron magnet. The magnetic field was then measured with a low-drift integrating fluxmeter. In either case, the field calibrations were determined using nuclear magnetic resonance.

Consistently, satisfactory bonds between the 20-MHz X-cut quartz transducers, the copper crystal, and the Z-cut quartz delay rod were produced using a mixture of about 3 parts glycerine to 1 part dimethyl sulfoxide (DMSO). These bonds were semipermanent in that they could be warmed and reused almost indefinitely (for a month or more) with no apparent signal deterioration, yet they could be readily slid apart when slightly warmed. In the bonding procedure, the components were carefully cleaned and warmed, then wet with a minimum quantity of the liquid and assembled under light spring pressure. If the transmitted signal was satisfactory at room temperature, the bonds were invariably sound on cooling to liquid-helium temperature. The proportions of the ingredients of the cement appear to be noncritical; however, essential to the success of the method is a slow cooling and warming rate with the avoidance of any thermal shock. All crystals were grown from American Smelting and Refining Co. (ASARCO) 99.999+grade copper. The ingots were aligned by x-ray back-reflection techniques and specimens were prepared by electrical discharge machining to minimize mechanical strain. The surfaces were planed and fine finished with an Agietron model AB unit with a model 30 H pulse-type power supply. No further hand polishing was found necessary to obtain consistently good ultrasonic echoes.

Different preparation techniques were used for the various crystals. The specimen on which the {100} data here reported was obtained was grown at Naval Research Laboratory by the Bridgeman technique and annealed for one day at 900°C in air at a pressure of 5×10^{-4} mm Hg by the procedure outlined by Gniewek and Clark.[17] The residual resistivity ratio (RRR) between room temperature and 4.2°K was 1000 before anneal and between 6000 and 7000 afterward. All of the other crystals were grown by Research Crystals, Inc., Richmond, Va., using the Czochralski method. The specimen on which the most detailed {110} data was obtained was also annealed as described above. The initial RRR was about 2500 and final about 8000. Sharper open-orbit resonances and more oscillations were obtained on {110}, {111}, and {112} specimens which had undergone a slightly different treatment. In these cases, annealing at 1000°C for five days was done after slicing but before planing. Oxygen at a pressure of about 1.2×10^{-4} mm Hg was used rather than air. The measured RRR are on the order of 11 000 and, typically, about 50% more oscillations were observed.

Although the copper Fermi surface is relatively simple in form, at most magnetic field angles and particularly at high fields many oscillation frequencies are mixed in the magnetoacoustic data. In general, the limited mean free path and other effects which reduce the amplitude confine the high-frequency oscillations to the high-field region, while at lower-fields lower-frequency components persist. This permits a separation of the various frequencies to be accomplished by a graphical analysis. When all frequencies clear enough to be distinguished were sorted out, each could be associated with a definite Fermi-surface orbit and feature. There was no evidence of frequencies which are sums and differences of other components. It was possible to distinguish extremal and nearly extremal regions, central and noncentral orbits, open and closed orbits, and, where the periodicity of an open orbit in real space had a component in the direction of the sound wave, sharp open-orbit resonances. The mixing of components at high fields usually made it impractical to attempt a determination of a phase angle which otherwise would have helped to distinguish between open and closed orbits and to suggest the curvature of regions giving rise to oscillations.

There exist a number of useful guides to orbit identification: Open-orbit resonances are readily identified as a series of sharp attenuation peaks often superimposed on an oscillation pattern but occurring only very close to symmetry directions and exhibiting zero phase. Oscillations of large amplitude suggest broad extremal regions on the Fermi surface and a large proportion of contributing electrons. An extended series of oscillations suggests an extremal region, while an unusually damped train suggests nonextremal or nearly extremal regions. Many orbits have a center of symmetry, sometimes at the zone center Γ. When a radial dimension does not fit the model, the center of symmetry may lie at other points in the Brillouin zone, such as X or L. A correct identification yields a self-consistent form for the surface.

III. EXPERIMENTAL RESULTS

A. Estimates of Mean Free Path

The mean free path l can be derived in several ways; from the number of observed oscillations, from the decay in amplitude of these oscillations, from the measured residual resistivity, and from the sharpness of the open-orbit resonances. Each method gives comparable results when applied to the same copper specimen having a RRR of 8000. For sound propagated along the $[01\bar{1}]$ direction and magnetic field near [100], belly orbits produce a particularly strong unmixed oscillation

[17] J. J. Gniewek and A. F. Clark, J. Appl. Phys. **36**, 3358 (1965).

pattern. The oscillations at higher fields have the pronounced scalloped structure characteristic of a Fermi surface having a right cylindrical form,[6] and the decay of oscillation amplitude is regular until the oscillations are lost in the system noise. In all, a train of about 70 oscillations at 476 MHz can be counted for the specimen with this RRR. A number so defined is not a well-specified quantity but has commonly been used to provide a rough measure of ql, since the number of observable oscillations is proportional to ql. Kjeldaas and Holstein[18] show that for a free-electron model with a finite mean path a value of $ql=10$ corresponds to about four clearly observed oscillations. On that basis, 70 oscillations is equivalent to $ql=175$ and $l=0.03$ cm. The regular decay of the oscillatory component of the attenuation α for this same series of oscillations is well accounted for by an initial geometric decay factor $n^{-1/2}$ and an exponential $e^{-n\pi\lambda/l}$, after the manner of Bohm and Easterling.[15] The value for mean free path derived from this analysis is $l=0.023$ cm.

The Fermi surface of copper is close enough to a sphere that a correlation would be expected between the electron mean free path as calculated from the low-temperature residual resistivity ρ and as determined from belly-type orbits (central orbits around the body of the Fermi surface). This proved to be the case. For a free-electron model, the mean free path l is given by $l=mv/Ne^2\rho$, where N is the density of free electrons, m is the electron mass, and v is the Fermi velocity. If an effective Fermi velocity 0.71 of the free-electron value is used, as indicated for belly orbits with $\mathbf{H}\|\langle 100\rangle$ in copper by the cyclotron resonance data of Koch, Stradling, and Kip,[19] the mean free path for a resistivity ratio of 8000 is, by this model, approximately 0.027 cm and the value of ql at 500 MHz is 170. The open-orbit resonances are also useful in providing an estimate of the mean free path.[6,20–22] The complexity and the mixture of frequencies in the oscillation patterns make it difficult to meaningfully correlate the attenuation at resonance with the attenuation at zero field, but the width of the resonance between points where the open orbit contribute has dropped to one-half the maximum value is a convenient measure. This width, according to Galkin, Kaner, and Korolyuk,[21] is given by $\Delta H/H=\frac{1}{2}ql$ and is independent of the order n of the resonance. A series of eight resonances could be distinguished for this same $\{110\}$ specimen with the magnetic field perpendicular to a $\langle 111\rangle$ direction. The relative width $\Delta H/H$ for $n=1$ yields $ql=190$ and for $n=4$, $ql=160$, and, correspondingly, the mean free paths $l=0.032$ and $l=0.027$, respectively. These results are comparable to those from the other methods.

B. Velocity of Sound

For a preliminary analysis of the experimental data, longitudinal velocities of sound in the principal directions were calculated from 0°K elastic moduli as tabulated by Overton and Gaffney.[23] A density of 0.9023 was assumed, consistent with an atomic weight of 63.54 and a lattice constant at 4.2°K of 3.603×10^{-8} cm. These velocities, essentially the same as used by Bohm and Easterling,[15] are 4.420×10^5 cm sec^{-1} for the [100] direction, 5.075×10^5 cm sec^{-1} for the [110] direction, 5.275×10^5 cm sec^{-1} for the [111] direction, and 5.114×10^{-5} cm sec^{-1} for the [112] direction. It was found that, with these velocities, the results disagreed when the same Fermi-surface contour was measured from two different symmetry points, e.g., from Γ and X or from Γ and L. Furthermore, the dimensions derived from the periodicity of open-orbit resonances fell short of the appropriate Brillouin-zone spacings which they should almost equal. However, the magnetoacoustic measurements became internally consistent when the velocities were adjusted to match the open-orbit data with the Brillouin-zone dimensions. This required a correction consistently much larger than the margin of 0.1% cited by Overton and Gaffney.

Extensive series of open-orbit resonances were observed in copper single crystals oriented for sound propagation in the $\langle 110\rangle$, $\langle 111\rangle$, and $\langle 112\rangle$ directions. Knowing the field B at resonance and the ultrasonic frequency ν, the velocity of sound may be determined from the relation $v_s=chk\nu/nBe$, where n is the order of the resonance. For example, for $\mathbf{q}$ along $[01\bar{1}]$ and $\mathbf{B}$ perpendicular to the [111] open-orbit direction, the open-orbit repeat distance and Brillouin-zone spacing ka is $2\sqrt{3}\pi$. From a series of 10 resonances (with the purer specimen) which could be precisely measured, a sound velocity of $5.10_7\times10^5$ cm sec^{-1} was determined. Similarly, for $\mathbf{q}$ along $[\bar{1}1\bar{1}]$ with $\mathbf{B}$ perpendicular to the [011] direction, the average of nine sharp resonances gave a sound velocity $5.31_9\times10^5$ cm sec^{-1}. Some measurements were also made with a sound direction $\mathbf{q}$ along $[\bar{1}1\bar{2}]$. Slant open orbits occur along $[11\bar{1}]$ and [010] and equivalent symmetry directions. Eight directions in all were examined with four to nine resonances each for a sound frequency of 622 MHz. The velocity of quasi-longitudinal waves for the $[\bar{1}1\bar{2}]$ direction was found to be $5.17_2\times10^5$ cm sec^{-1}. For a sound wave along a [001] direction, the positions of the necks preclude open-orbit resonances; however, open orbits in the [001] direction are possible for fields slightly displaced from [110], and they gave a prominent set of oscillations. Their dimension extrapolated to the $[\bar{1}10]$ direction (see Fig. 1) matches the Brillouin-zone spacing and, thus, provides

[18] T. Kjeldaas and T. Holstein, Phys. Rev. Letters **2**, 340 (1959).
[19] J. F. Koch, R. A. Stradling, and A. F. Kip, Phys. Rev. **133A**, 240 (1964).
[20] B. C. Deaton and J. D. Gavenda, Phys. Rev. **136**, A1096 (1964).
[21] A. A. Galkin, E. A. Kaner, and A. P. Korolyuk, Zh. Eksperim. i Teor. Fiz. **39**, 1517 (1960) [English transl.: Soviet Phys.—JETP **12**, 1055 (1961)].
[22] C. W. Burmeister, D. B. Doan, and J. D. Gavenda, Phys. Letters **7**, 112 (1963).
[23] W. C. Overton, Jr., and J. Gaffney, Phys. Rev. **98**, 969 (1955).

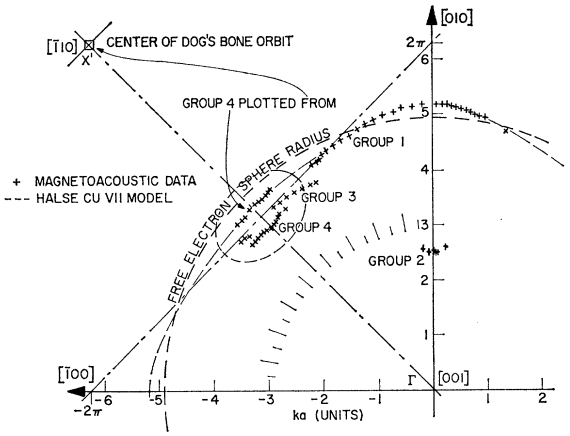

FIG. 1. Fermi surface of copper in a (001) projection, $\mathbf{q}\|[001]$. The experimental dimensions determined from the period of magnetoacoustic oscillations for **B** in the (001) plane are plotted as if from a common center Γ. Group 4 is also replotted from the center of the dog's bone orbit X'. The scale is in units of ka, where k is the magnitude of the sound-wave vector and a is the cubic-lattice constant for copper.

the means of standardization of the other oscillations. The sound velocity inferred for the [001] direction is $4.46_5\times10^5$ cm sec^{-1}.

The small but significant increments observed from velocities of sound calculated from the elastic moduli[23] to those inferred from these magnetoacoustic results may have their origin in several effects, each of which would increase the apparent velocity. These include transducer corrections to the measurement of elastic moduli, differences in specimen preparation and in physical treatment given the copper single-crystal specimens, and the substantial difference in frequency (a factor of about 50) between the pulse-echo modulus measurements and the magnetoacoustic experiments. The effects will be discussed in turn.

Transducer corrections. Overton and Gffney[23] carefully considered the effect of the bonding layer between the transducers and the specimen, but not the effects of acoustic mismatch between the quartz and copper and the resulting transit-time error associated with the finite thickness of the quartz transducers. Kammer[24] has developed a technique which corrects for this effect by extrapolating the measured sound velocities to zero transducer thickness. An application of his analysis to the experimental conditions suggests a correction of about +0.45% to their measured velocities.

Specimen preparation differences. The magnetoacoustic specimens were prepared by electrical discharge machining with a low-spark intensity setting to minimize strain. The specimens for elastic modulus measurements had been prepared by lathe machining after being oriented and waxed into molds. While no significant strain may have been introduced by this process, the presence of strain can influence the elastic moduli as is illustrated by the observations of Alers and Thompson.[25] They found that a copper single crystal given a 1% uniaxial strain and allowed to recover, though not actually annealed, showed a reduction of 0.3% in longitudinal velocity when measured at 4.2°K. The single crystals for elastic modulus measurements had been grown in graphite molds in a helium atmosphere, i.e., in the absence of oxygen. In contrast, the magnetoacoustic specimens had all undergone an extended oxygen annealing treatment. This increases the apparent purity when measured in terms of the electron mean free path, but is known to produce precipitate particles of cuprous oxide within the crystals and, associated with them, clusters of dislocations.[26] If this modification of the structure should measurably change the lattice constant, and, thus, the density, it would thereby affect the acoustic velocity.

Dispersive effects. Alers and Thompson demonstrated that the motion of dislocations produces a measurable decrease in the velocity of sound at the frequency at which the elastic moduli had been measured (10 MHz). They removed this dislocation contribution by neutron irradiation and showed that, for longitudinal waves in copper, the magnitude of this effect is on the order of 0.15% in the velocity. Frictional forces and inertia at the very high frequencies of these magnetoacoustic experiments typically remove this dislocation contribution, as was shown by Granato and Lücke.[27]

There is a dependence of the velocity of sound on the electronic component of the acoustic attenuation. The effect is enhanced for very pure metals at high frequencies and, furthermore, is field-dependent. It has been studied both theoretically and experimentally,[28,29] and may be significant under the conditions of the present experiments. The velocity changes to be expected for copper at zero magnetic field may be calculated using the orientation and frequency dependence of acoustic attenuation found by MacFarlane, Rayne, and Jones.[30] The increase of velocities to be expected under the assumption of a mean free path of 0.03 cm at a frequency of 500 MHz are 0.08% in the ⟨100⟩ direction, 0.03% in the ⟨110⟩ direction, and 0.07% in the ⟨111⟩ direction. The acoustic attenuation changes relatively little for copper except at high magnetic fields, but there the accompanying velocity change may shift the locations of the magnetoacoustic oscillations and of the open-orbit resonances. Under the same assumptions as above, the maximum (infinite field) field-dependent

[24] E. W. Kammer, J. Acoust. Soc. Am. **37**, 929 (1965).

[25] G. A. Alers and D. O. Thompson, J. Appl. Phys. **32**, 283 (1961).

[26] F. W. Young, Jr., in *Direct Observation of Dislocations in Crystals*, edited by J. B. Newkirk and J. H. Wernick (Wiley-Interscience, Inc., New York, 1962), pp. 103–113.

[27] A. V. Granato and K. Lücke, in *Physical Acoustics*, edited by W. P. Mason (Academic Press Inc., New York, 1966), Vol. IV, Part A, Chap. 6, pp. 225–276.

[28] S. Rodriguez, Phys. Rev. **130**, 1778 (1963).

[29] B. G. Yee and J. D. Gavenda, Phys. Rev. **175**, 805 (1968).

[30] R. E. MacFarlane, J. A. Rayne, and C. K. Jones, Phys. Letters **19**, 87 (1965).

shift expected on a spherical Fermi-surface model[5] is 0.6%, but at the fifth oscillation is already found to be on the order of 0.06%. Experimentally, the first few open-orbit resonances are found displaced to lower fields by several tenths of a percent compared to the remainder of the series. In the determination of velocities from open-orbit resonances, such clearly displaced resonances were omitted.

Except for the field-dependent velocity effects discussed, the use of open-orbit resonances as a reference avoids the necessity of making corrections to the velocities obtained from the elastic moduli. The inclusion of corrections for electronic attenuation, for dislocation motion, and for transducer transit time, however, bring the velocities derived from the elastic moduli into much better agreement with the magnetoacoustic results. Finally, it may be stated that the Fermi-surface radii calculated using velocities obtained through open-orbit resonances are in much better agreement with the analytical model of Halse (Cu VII).[11]

C. $\mathbf{q}\|\langle 100\rangle$

For the specimen with $\mathbf{q}\|\langle 100\rangle$, 40 complete oscillations could be observed for a sound frequency of 476 MHz in typical directions. This provided sufficient detail to allow an unambiguous assignment of oscillation frequency components to particular electron orbits. Within the angular range where electrons can travel in central orbits entirely around the Fermi surface, the so-called "belly-orbit" oscillations (group 1 in Figs. 1 and 2) are observed. For a direction within 2° of [010], secondary oscillations are superimposed, yielding dimensions which match very well those expected for the "4-cornered rosette orbits" (group 2 in the figures). This orbit passes through four connecting necks and four adjoining zones in the extended zone scheme, as illustrated. Between 5° and 15° of $[\bar{1}10]$, strong oscillations arise from open orbits traveling in the [001] direction (group 3 in the figures). By this identification, it is seen from Fig. 2 that the dimension near $[\bar{1}10]$, where the open orbit is blocked by the necks, approaches the Brillouin-zone dimension $\sqrt{2}\pi$ and, therefore, provides a convenient calibration. This was then used for all of the other oscillations. On this face, although there were no open-orbit resonances which could serve as standards independent of the sound wavelength, it was still possible in this manner to utilize an internal standard. Near $[\bar{1}10]$, very strong oscillations are observed at high fields, as illustrated in Fig. 3. In the literature, these are ascribed to the "dog's bone" orbit, which is quite natural since the dog's bone is the extremal orbit for this direction. With the added resolution achieved in these experiments, it became obvious that the true dog's bone oscillations (group 4 in Fig. 1 and 2) are observable only at low fields and only within a restricted angle, about $\pm 6°$ of the symmetry direction. It was discovered also that the low-field and the high-field oscillations yielded distinctly different dimensions. The strong masking oscillations at high fields show no break at angles where a dog's bone interpretation becomes impossible; in fact, they persist out to $\pm 20°$. They must, therefore, be ascribed to a wide band of off-center nearly extremal belly-type oribts (group 5 in Fig. 2). The oscillations at high fields are damped rapidly, and the break between high-field and low-field patterns is visible in Fig. 3.

In Fig. 1, the groups of magnetoacoustic dimensions are compared with a free-electron sphere and with the analytic model of Halse (Cu VII). The dimensions from

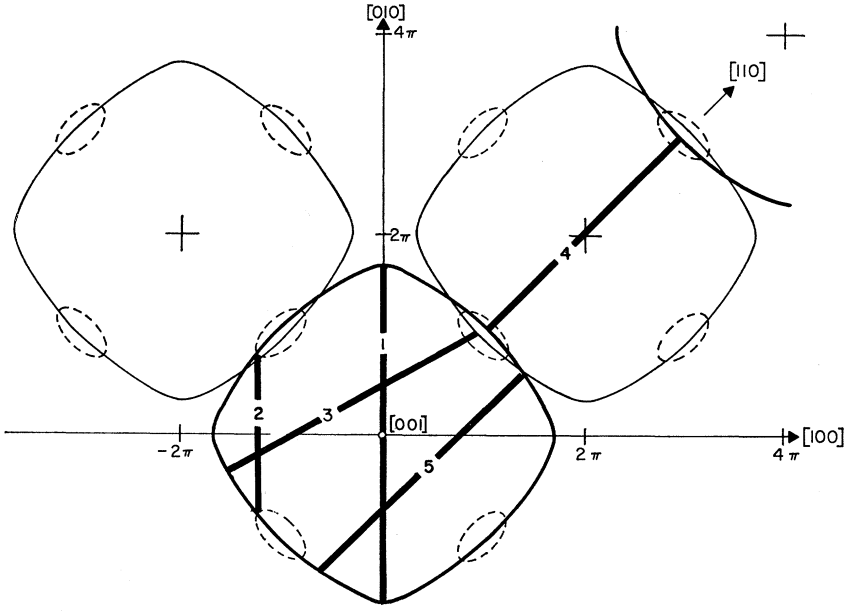

FIG. 2. Location of orbits associated with magnetoacoustic oscillations observed with $\mathbf{q}\|[001]$. To simplify the presentation the extended-zone scheme is used. The ellipses are projections of the intersection of necks with the Brillouin-zone faces. The orbits shown are typical. Actual oscillations are observed over a range of angles determined principally by the neck locations.

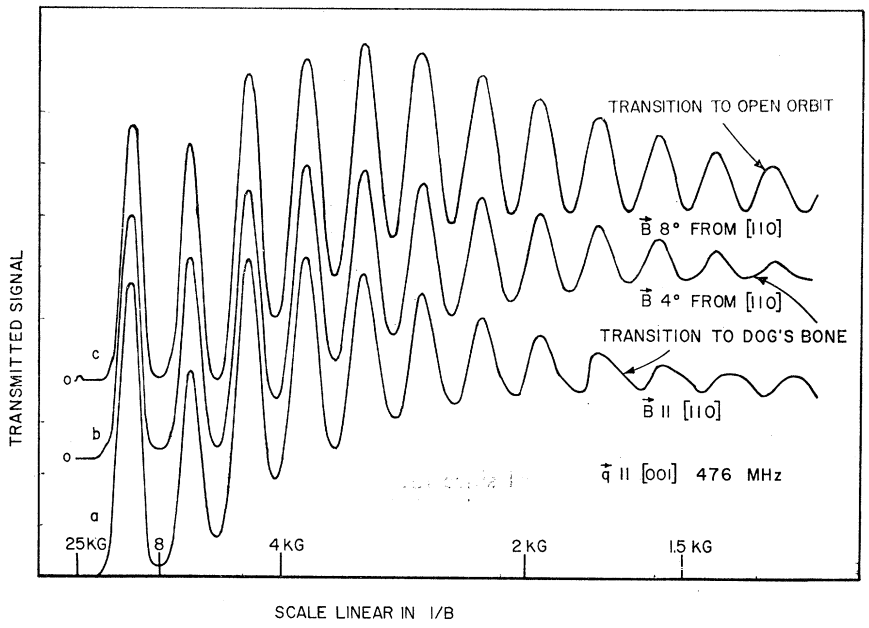

FIG. 3. Rapidly damped high-field portion of the oscillation pattern for $\mathbf{q}\|[001]$ with $\mathbf{B}\perp[\bar{1}10]$ and rotated by 4° and 8°. The oscillations represent nonextremal orbits, specifically off-center belly orbits, but have previously been incorrectly called dog's bone oscillations. Nearly unchanged in form, they persist to rotation angles up to 20°, whereas an absolute maximum of 10° is dictated by the neck diameter. At lower fields, oscillations from extremal orbits, which begin to show at the right side of the figure, persist and yield distinctly different dimensions. The actual dog's bone oscillations are seen up to 6°.

oscillations at lower fields, here ascribed to the true dog's bone orbits (group 4 in Figs. 1 and 2), are shown radially as if from point Γ and as replotted from the dog's bone center, point X'. The replotted points match fairly well with the (Cu VII) outline, thus strengthening this interpretation.

An estimate, though not a true measurement, of the neck radius is possible from the rosette orbit dimension in the [010] direction. Approximately, the neck radius is equal to the product of $\sqrt{2}\pi$ and the rosette radius. The value so obtained is 0.91. Smoothed dimensions at 5° intervals for groups 1–3 and 5 are presented in Table I.

TABLE I. Smoothed magnetoacoustic dimensions for copper with $\mathbf{q}\|\langle 100\rangle$ at 5° intervals. An angle of 0° corresponds to a $\langle 100\rangle$ direction on the Fermi surface, while 45° corresponds to a $\langle 110\rangle$ direction. The units of the tables, as well as those in the figures, are dimensionless units of ka, where a is the cubic lattice constant for copper, taken as 3.603×10^{-8} cm, and $\hbar k$ is the electron momentum. In these units the distance from Γ to X is 2π and from Γ to L is $\sqrt{3}\pi$. For comparison, the free-electron radius is $(12\pi^2)^{1/3}\cong4.91089$.

Angle from $\langle 100\rangle$	Fermi-surface radii composite of groups 1 and 4 of Figs. 1 and 2	Rosette group 2	Open-orbit group 3	Off-center belly-orbit group 5
0°	5.18	2.50	...	...
5°	5.13	2.58	...	...
10°	5.03	...	...	...
15°	4.92	...	...	...
20°	4.80	...	...	...
25°	4.71	...	...	5.00
30°	4.65	...	4.33	4.44
35°	...	...	4.375	4.40
40°	4.67	...	4.42	4.37
45°	4.69	...	$\sqrt{2}\pi$ (standard)	4.35

Group 4, the dog's bone, is considered as plotted from its appropriate center and combined with group 1 as Fermi-surface radii.

D. $\mathbf{q}\|\langle 110\rangle$

The specimen on which the most extensive data was taken was cut from a Czochralski-grown annealed crystal. The measurements at 476 MHz were taken at 2° intervals. The data were supplemented by very careful measurements at 670 MHz on a crystal which had been oxygen annealed after slicing. Figure 4 summarizes the magnetoacoustic data and Fig. 5 identifies the origin of the various groups into which the data fall. The location and extent of these groups is mainly determined by the neck regions. The Fermi-surface outline shown in dashed lines is the central cross section according to the analytic model of Halse (Cu VII). For clarity, the neck intersections with the Brillouin zone are shown as ellipses, though these do not lie in the central plane. The dimensions found range from some much smaller than the radius of the necks to others much too large to indicate on the figure. This is possible within the accepted model because small extremal regions of larger orbits are observable and because the existence of necks permits greatly extended orbits at some angular ranges. To the scale of Fig. 4, the deviation of the dimensions from the model of Halse (Cu VII) is not evident; however, the deviation from the model of Roaf (Cu VI) is appreciable.

Groups 1a and 1b are the most prominent oscillations observed and represent the belly orbits passing entirely around the surface within one zone. Near 0°, the [011] direction, the large oscillations are scallop-shaped with peaks which are more resonant than harmonic. Here,

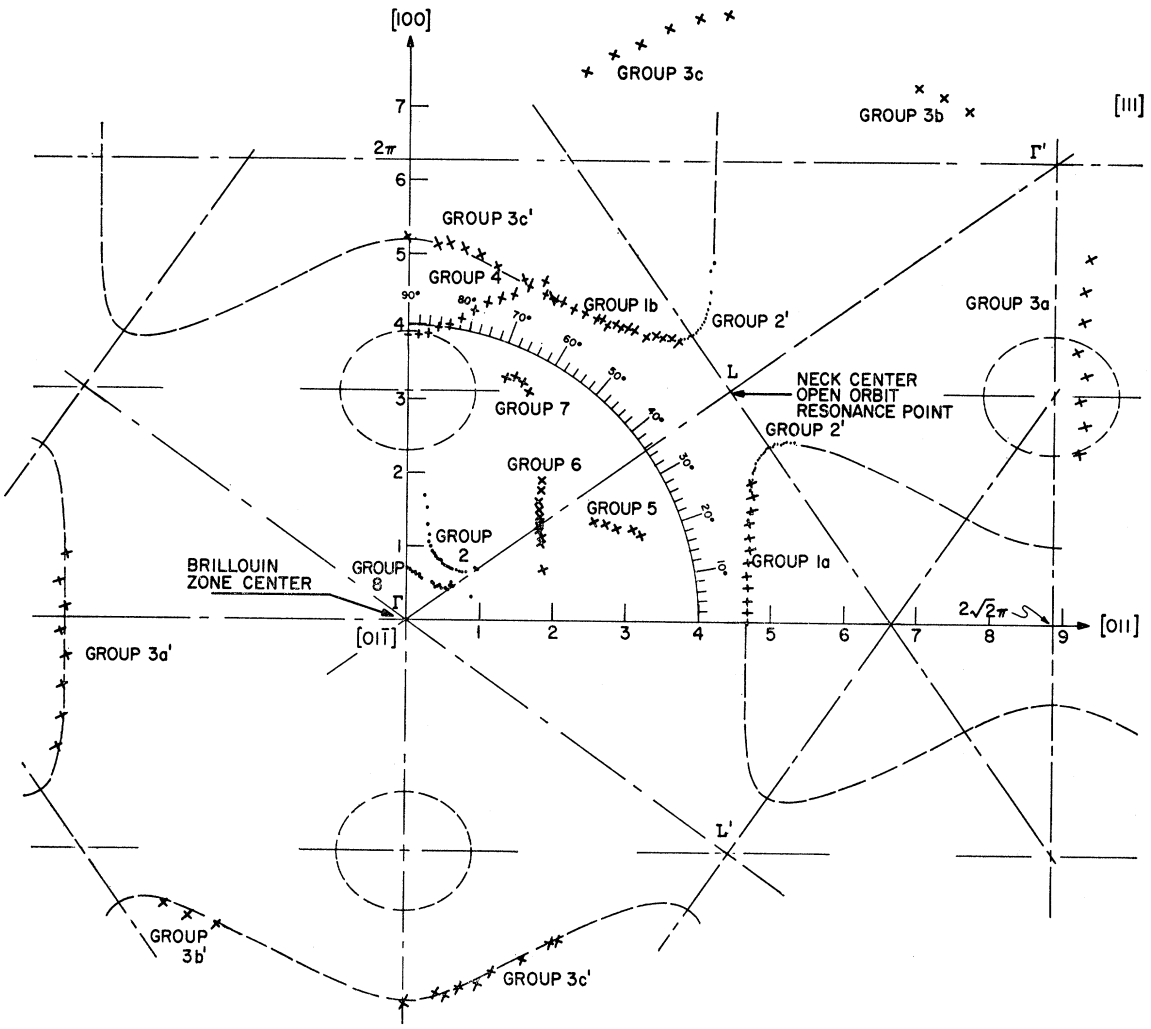

FIG. 4. Magnetoacoustic dimensions measured with $\mathbf{q}\|[01\bar{1}]$. Where primed, the dimensions have been replotted from the neck center L or L' rather than from the original Γ to clarify the interpretation. The dashed lines indicate the analytic model Halse (CuVII). The scale is in dimensionless units of ka. Dimensions are referenced to the open-orbit resonance point at L for which $ka=\sqrt{3}\pi$.

100 complete oscillations could be counted for the purest specimen. The dimensions of groups 1a and 1b clearly measure the central cross section of the surface. The oscillations become weaker near the [111] and [100] directions and no longer occur where necks block such orbits. The dimensions of group 2 measure the neck regions directly. The oscillations are relatively weak, but with care can be separated from the others. When the dimensions are replotted as group 2′ from a neck center L rather than from Γ, their interpretation becomes obvious. The dimensions of groups 3a, 3b, and 3c are larger than a Brillouin zone. Like group 2, their interpretation becomes obvious when they are replotted as groups 3a′, 3b′, and 3c′ from a neck center L or L'. These dimensions measure the extent of dumbell-shaped orbits passing through two zones. The group 3c′ is particularly interesting because it gives a measure of the surface contour near the $[\bar{1}00]$ direction where belly orbits have been blocked by the necks. The dimensions and form in this region match the results from the {100} specimen.

The dimensions in group 4 may be understood with reference to Fig. 5 as arising from off-center orbits which pass around two necks. The dimension at 90° matches that which would be obtained from group 2′ by this interpretation and, thus, provides a check on both interpretations. The orbit path for group 5 is off-center around a single neck. It is mostly within a single zone, but for a short distance passes, like the neck orbits of group 2, into the adjacent zone. The angular range, as well as the dimensions, are consistent with this interpretation. Group 6 and a portion of group 8 can be explained as arising from a family of open orbits traveling in the $[01\bar{1}]$ direction by way of a chain of necks. This path has a doubly reentrant form with a repeat distance of $4\sqrt{2}\pi$ and for the ⟨111⟩ direction has been seen as an

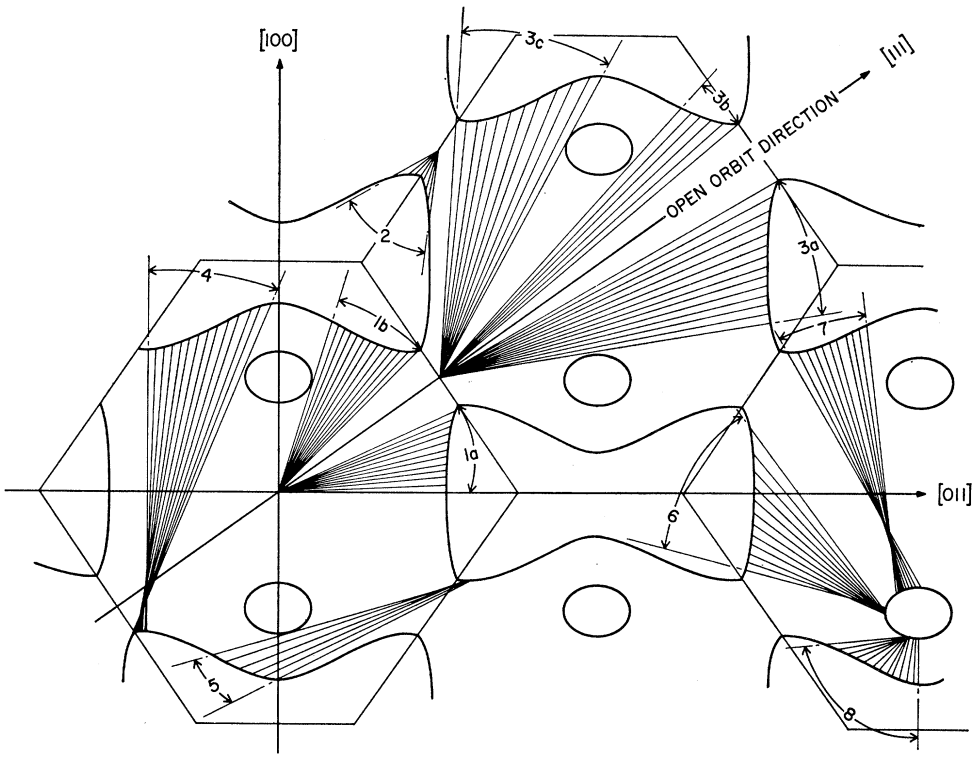

FIG. 5. Fermi surface of copper in an extended-zone space projected onto a $(01\bar{1})$ plane with the angular ranges of the principal magnetoacoustic orbits indicated, corresponding to the dimensions of Fig. 4. The orbits having a center of symmetry, groups 1a, 1b, 2, 3a, 3b, and 3c, are indicated radially. The other more complex orbits, groups 4–8 are indicated between their two extremal regions. The lines shown indicate the location and angular range of the orbits and not the angles of actual measurement.

open-orbit resonance on the {111} face. A similarly shaped orbit gives rise to group 7 and another portion of group 8.

TABLE II. Smoothed magnetoacoustic dimensions for copper with $\mathbf{q}\|\langle 110\rangle$ at 5° intervals. An angle of 0° corresponds to a $\langle 110\rangle$ direction on the Fermi surface, while 90° corresponds to a $\langle 100\rangle$ direction. Dimensions are given in units of ka and are standardized to make the distance from Γ to L as measured by open-orbit resonances equal to $\sqrt{3}\pi$.

Angle from $\langle 110\rangle$	Fermi-surface radii, a composite of groups 1–3 of Figs. 3 and 4	Neck caliper dimensions group 2
0°	4.69	···
5°	4.71	···
10°	4.76	···
15°	4.86	···
20°	5.02	···
25°	5.39	···
30°	contact	···
35°	contact	···
40°	contact	1.07
45°	5.50	0.99
50°	5.09	0.94
55°	4.93	0.925
60°	4.84	0.935
65°	4.82	0.975
70°	4.90	1.045
75°	4.96	1.18
80°	5.05	1.56
85°	5.14	···
90°	5.18	···

The points of group 6 in Fig. 4 lie on a vertical line, suggesting that this is an image of group 1a. The angular range and the dimensions are consistent with this interpretation. This identification provides a means of measuring the neck radius in a $\langle 110\rangle$ direction. Since the surface outline is very straight over the range of angles over which group 6 is observed, twice the average projection in the [011] direction (3.74), subtracted from the surface radius in the same direction (4.69), yields a measure of the neck radius in the [110] direction (0.95). This value is consistent with the same radius obtained by a very similar process from data obtained for $\mathbf{q}\|\langle 111\rangle$, (0.93_8). Both appear to be larger than the radius (0.93) in a $\langle 112\rangle$ direction obtained from group 2. Strong open-orbit resonances are seen at the [111] direction where a series of 8 or more of them can be measured. Their amplitude and sharpness fall off rapidly at angles more than $\pm 1°$ of the symmetry direction. Again, the caliper or repeat dimension from those orbits has been set equal to the Brillouin-zone spacing of $2\sqrt{3}\pi$ and used as a standard for the data. For angles near those for which open orbits are possible electrons may follow extended orbits over several necks and return again in a closed path. The dimensions from orbits passing through successively larger numbers of zones are easily identified in the data but have not been included

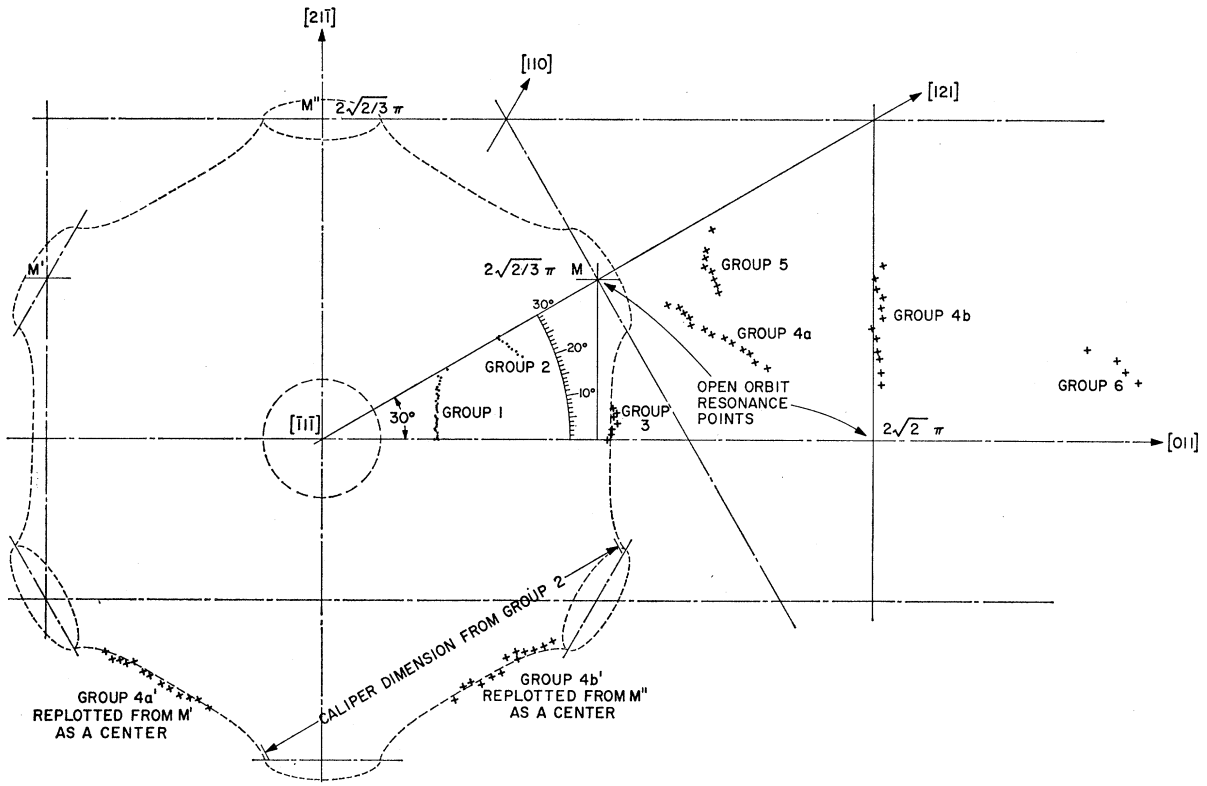

FIG. 6. Magnetoacoustic dimensions measured with $\mathbf{q}\|[111]$. All data points are plotted as if within the symmetry angle 0°–30°. Points M, M', and M'' are projections of neck centers L of hexagonal faces of the Brillouin zone onto the $(1\bar{1}1)$ plane. Groups 4a and 4b have been replotted from M' and M'', respectively, to clarify their interpretation. The dashed lines indicate the projections of the analytic model Halse (Cu VII). Note that the calipered extremal regions lie on the projection and not on the central section. As with the other figures, the dimensions are given in units of ka, in this case referenced to the open-orbit resonance point in the [011] direction at $ka=2\sqrt{2}\pi$.

in Figs. 4 and 5 because they do not yield any essentially new information. Smoothed dimensions for the principal groups are presented at 5° intervals in Table II.

E. $\mathbf{q}\|\langle 111\rangle$

The specimen on which the best data were obtained was prepared from a Czochralski-grown crystal and annealed as a thin slice in a partial pressure of oxygen. With a sound frequency of 579 MHz, two series of sharp open-orbit resonances were observed. One series, with 13 evenly spaced peaks visible, arises from an open orbit in the [011] direction with a repeat distance of $4\pi\sqrt{2}$ (see Figs. 6 and 7). This dimension was chosen as a standard for all other magnetoacoustic dimensions on this face. The other open-orbit resonance series at 30°, with three sharp peaks visible, arises from an open orbit in the [100] direction which lies out of the $(\bar{1}11)$ plane, but has a component in the plane in the $[21\bar{1}]$ direction with a repeat distance of $4\pi\sqrt{\frac{2}{3}}$. This latter orbit is particularly interesting because its real space direction is inclined 34.7° from $\mathbf{q}$ and electrons on this open orbit would leave the sound beam if the thickness were sufficient. The ratio of the repeat distances was within 1% of the expected geometric factor $\sqrt{3}$. The open-orbit resonances for the [011] direction are less sensitive to any slight alignment error and there are more such open-orbit resonances. For these reasons they are chosen as the standard for the interpretation of the magnetoacoustic oscillations.

Apart from the open-orbit resonances, six separate groups of oscillations were resolved. Over the full range, except narrowly near 30° (the [121] direction), the orbits of group 1 in Figs. 6 and 7 gave a strong oscillation pattern. They are open orbits in the $[\bar{1}1\bar{1}]$ direction and the oscillations measure the distance from the neck to the surface outline. The points lie very nearly in a vertical straight line, which is the projection of the Fermi-surface outline in the $(\bar{1}1\bar{1})$ plane. The orbit paths, as shown in Fig. 7, are nearly radial, not from the neck center, but from the neck radius in the [011] direction. The projection of these points on the [011] axis provides, as did a similar projection of group 6 for $\mathbf{q}\|\langle 110\rangle$, a measure of the neck radius in the [110] direction. Twice this projection (3.73) subtracted from the Fermi-surface radius in the [110] direction (4.69) yields the neck radius in the [110] direction (0.96). This measurement is consistent with the similarly obtained radius for $\mathbf{q}\|\langle 110\rangle$ of 0.95. These measurements are

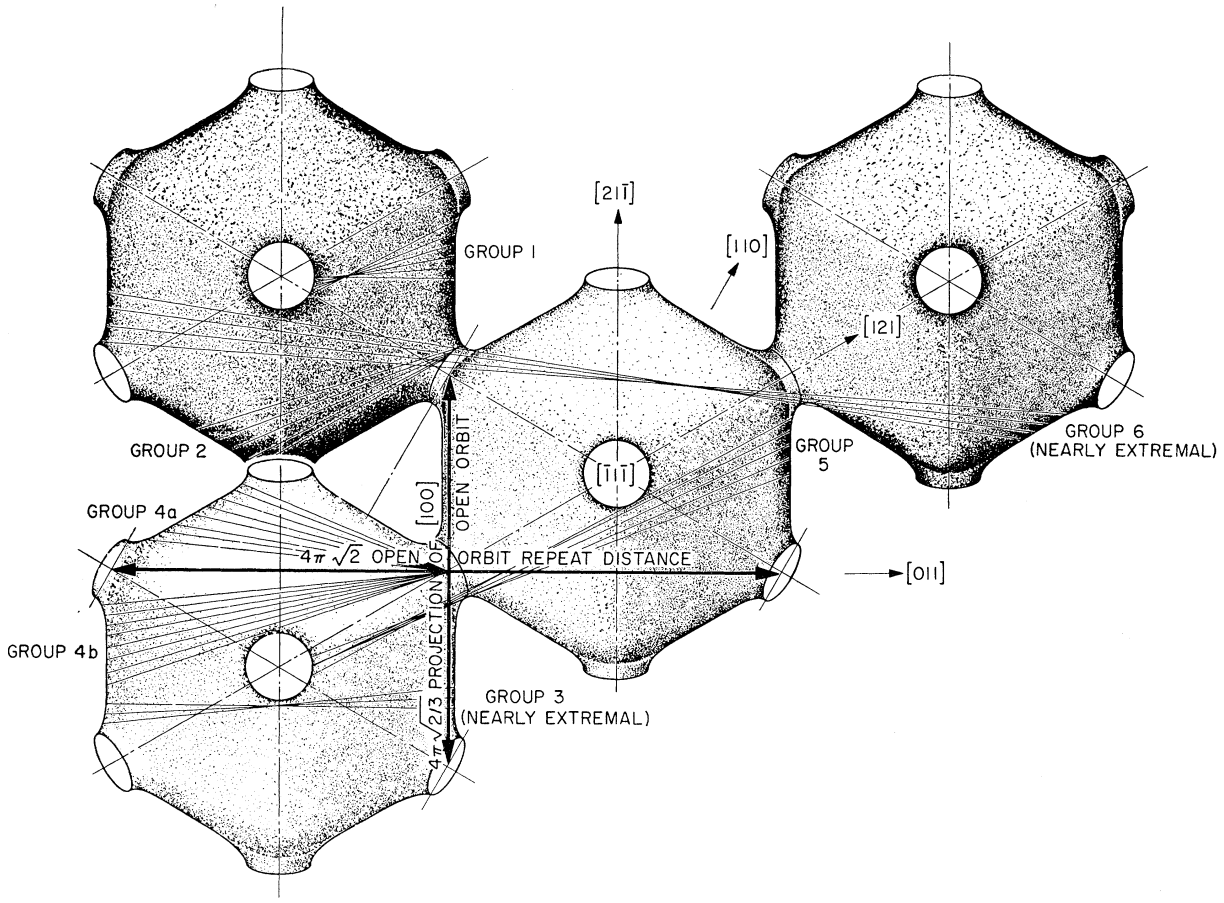

FIG. 7. Fermi surface of copper in a simulated three-dimensional projection of the extended-zone space on a ($\bar{1}1\bar{1}$) plane. Orbit-angular ranges are shown for the groups of Fig. 6. Groups 4a and 4b are shown radially, the others indicated between their calipered regions. Note that the belly orbits, group 3, are not centrally symmetric. Central belly orbits are blocked by the neck region and open orbits in the [$\bar{1}1\bar{1}$] direction occur instead.

higher than the directly measured ⟨112⟩ radius with $\mathbf{q}\|\langle 110\rangle$ (0.93_0) but equal within the experimental error. The much more accurate average-neck radius corresponding to the dHvA measurement of Jan and Templeton[25] is 0.9260. Oscillations from neck orbits were expected which would caliper the [110] direction directly, but none were found strong enough to measure with the graphical method of analysis employed.

TABLE III. Smoothed magnetoacoustic dimensions for copper with $\mathbf{q}\|\langle 111\rangle$ at 5° intervals. An angle of 0° corresponds to a ⟨110⟩ direction on the Fermi surface, while a 30° angle corresponds to ⟨112⟩. Note that except in the symmetry directions ⟨110⟩, the dimensions represent projections rather than radii. Dimensions are in units of *ka*.

Angle from ⟨110⟩	Fermi-surface projection a composite of groups 4 and 2 of Figs. 5 and 6	Open-orbit group 1
0°	4.65	1.86
5°	4.665	1.87
10°	4.72	1.89
15°	4.81	1.925
20°	contact	2.00
25°	contact	2.10
30°	contact	...

Dimensions of group 2 measure the extent of an off-center inclined orbit over two necks as shown in Fig. 7. As indicated in Fig. 6, at 30° the caliper dimension as replotted is consistent with the neck contour as determined for the (110) face.

There are no central belly-type orbits as found on the {100} and {110} faces because such orbits would be blocked by the necks; however, at angles up to 6° from [011], off-center nearly extremal belly orbits, group 3, can be noted from Figs. 6 and 7. The outline of the surface can be obtained from orbits centered at a neck and extending through two zones. These are groups 4a and 4b. Their radial dimension is plotted centrally in Fig. 6 and replotted from appropriate neck centers as groups 4a′ and 4b′. It is important to note that the dimensions are those of the Fermi-surface projection and not of the central section as on the {100} and {110} faces where this distinction does not exist. Group 5 oscillations arise from complex open orbits in the [$\bar{1}1\bar{1}$]

direction which are probably extremal. Group 6 oscillations arise from closed orbits which are not extremal passing through 3 zones. The band of contributing electrons is severely restricted by the location of necks. Groups 1–3, 5, and 6 all lack a center of symmetry, which limits their direct usefulness in determining the Fermi-surface outline. Smoothed dimensional data for groups 1, 3, 4a, and 4b are presented at 5° intervals in Table III.

F. $\mathbf{q}\|\langle 112\rangle$

A limited series of measurements were made for this sound direction. The possible open orbits here are all slant. If the sound direction is considered as the $[11\bar{2}]$ direction, then open orbits in the [010], the $[1\bar{1}1]$, and the $[00\bar{1}]$ direction, and others related by symmetry, give open-orbit resonances at angles in the plane determined by their projections. Resonances from the first two types were combined to give the velocity of sound. Central-belly orbits allow a measure of the Fermi surface in the $[\bar{1}10]$ direction, giving a value of 4.68_8 in ka units or 0.955 of the free-electron sphere radius, matching the results with a $\langle 110\rangle$ sound direction and the radius calculated by Faulkner *et al.*, for their V_I potential model. The oscillations from this slant cylindrical region were no longer sharply cusped, though an equally long train was observed.

IV. CONCLUSIONS

Tables I–III present a summary of the magnetoacoustic dimensions at 5° intervals. Also included is a composite of groups which for Tables I and II give the Fermi-surface radii in the two principal planes and for Table III a projection of the surface. The nominal accuracy for the dimensions is $\pm 0.4\%$ of the free-electron radius. Table IV compares radii determined in this experiment with other experimental results, with several syntheses of dHvA frequencies, and with results of recent band-structure calculations. The model of Halse (Cu VII) is seen to be a much better fit to the magnetoacoustic results than that of Roaf (Cu VI). The model of Zornberg and Mueller yields dimensions slightly too large, as noted by the authors, but otherwise appears to be a close fit at all angles. The calculated model of Faulkner *et al.* for the potential V_I is an excellent fit to the experimental data except possibly at the neck. It is not possible within the accuracy of this experiment to distinguish whether the approximation $l_{\max}=4$ is a better fit than $l_{\max}=2$.

Related to cyclotron resonances, an effect with finite $\omega\tau$ has been described by Gavenda and Chang,[31] namely, a null and reversal of phase of the magnetoacoustic oscillations at a field twice that at which cyclotron resonance is to be expected. This should be observable under the conditions of this experiment, but no evidence of an effect was seen (cf. Fig. 8).

It became necessary to find an internal standard when the direct application of the available elastic moduli gave an inconsistent interpretation of dimensions. This was provided with copper by the open orbits. Typical open-orbit resonances are illustrated in Figs. 9 and 10. The number of corrections to the velocity of sound

[31] J. D. Gavenda and F. H. S. Chang, Phys. Rev. Letters **16**, 228 (1966).

TABLE IV. Comparisons of copper Fermi-surface radial dimensions in symmetry directions, expressed relative to the free-electron sphere radius.

Source	$\langle 110\rangle$ radius	$\langle 100\rangle$ radius	Neck radius
This work (magnetoacoustic)	0.95_5	1.05_5	0.18_9
Bohm Easterling (magnetoacoustic)	0.95_6	1.03_6	0.19_5
Jan and Templeton[a]	...	...	0.1886[b]
O'Sullivan and Schirber[c]	...	...	0.1886[b]
Halse (Cu VII) (Spherical harmonic expansion)	0.951	1.059	...
Roaf (Cu VI) (Spherical harmonic expansion)	0.943	1.076	0.200
Zornberg and Mueller (Cubic harmonic expansion)	0.958	1.060	0.190
	(KKR calculation)		
Faulkner *et al.*			
V_I $l_{\max}=2$	0.9553	1.0501	0.178
V_I $l_{\max}=4$	0.9544	1.0530	0.1808
V_{II}	0.9426	1.0658	0.2146
	(APW calculation)		
Snow and Waber			
Slater=1	0.939	0.998	0.161
Slater=$\frac{2}{3}$	0.836	1.056	0.279

[a] J. P. Jan and I. M. Templeton, Phys. Rev. **161**, 556 (1967).
[b] These average radii are derived from the measured dHvA frequencies assuming a circular cross section and a lattice constant of 3.603×10^{-8} cm. The precision of these frequencies is much higher than that of the magnetoacoustic measurements.
[c] W. J. O'Sullivan and J. E. Schirber, Cryogenics **7**, 118 (1967).

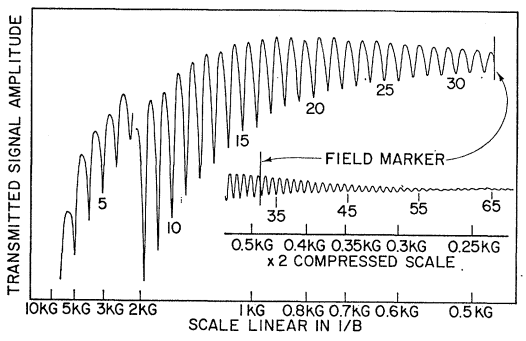

FIG. 8. Reproduction of the recorder tracings showing magnetoacoustic oscillations in copper for $\mathbf{q}\|[011]$ and $\mathbf{B}\perp[011]$ at a frequency of 476 MHz. The large amplitude and sharp attenuation peaks (the minima of the recorded trace) suggest that the extremal region is broad and cylindrical. Measurements at 670 MHz on another purer specimen showed more sharply resonant peaks and over 100 oscillations.

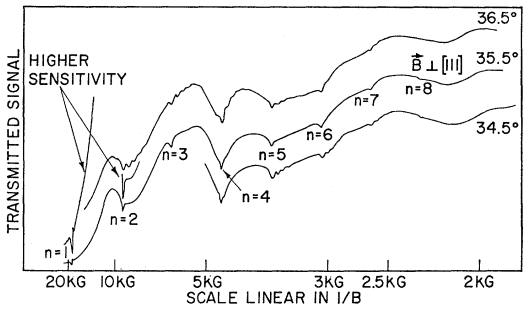

FIG. 9. Resonances from open orbits in copper at 476 MHz for $\mathbf{q} \| [01\bar{1}]$ and $\mathbf{B} \perp [111]$ and at angles $\pm 1°$ from the symmetry direction. Such resonances are used as a standard for the magnetoacoustic data, effectively providing an independent measure of the velocity of sound.

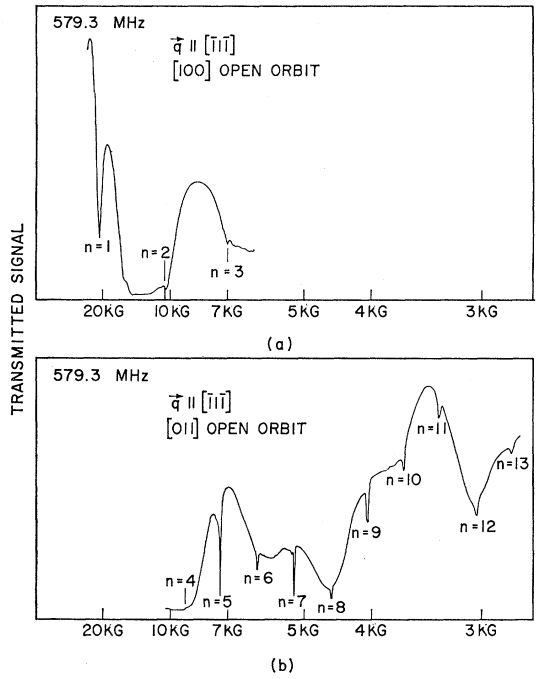

FIG. 10. Open-orbit resonances with $\mathbf{q} \| [\bar{1}1\bar{1}]$, as indicated in Fig. 6, superimposed on the magnetoacoustic oscillations. The shorter series measures the projection on the $(\bar{1}1\bar{1})$ plane of a slant open orbit in the [100] direction. The more extensive series is for an open orbit in the [011] direction (in the $[\bar{1}1\bar{1}]$ plane). The latter with a repeat distance of $4\pi\sqrt{2}$ was chosen for a calibration standard and also provided an independent measure of the velocity of sound in the $[\bar{1}1\bar{1}]$ direction.

which have been shown necessary if a high accuracy is desired suggests that the question is not so much "what is the velocity of sound?" as "which velocity of sound?"

A significant advantage of the magnetoacoustic method for Fermi-surface studies is that it yields dimensions directly. For very pure metals, the number of oscillations can be high enough to yield good precision and to distinguish the extremal regions. A limitation of the method is that the dimensions found are not always the desired radial dimensions but are, more generally, those projections of surface regions in the direction of the sound wave for which appropriate electron orbits exist. As a result, even a relatively simple Fermi surface such as that of copper having a single sheet yields a large number of frequencies which caliper both extremal and nearly extremal orbits, and a careful analysis of the data is, thus, required.

If measurements are made on copper specimens with a significantly higher purity (as has been achieved[32]) a better resolution of the frequencies could be realized and acoustic-cyclotron resonances would become clearly observable. With the higher ql, a correction would be necessary for the change in velocity with magnetic field. The accuracy could be further improved until the specimen thickness, dictated by system noise and the acoustic attenuation, limits the orbit size. If more frequency components are to be resolved, and, particularly, if metals with relatively complex Fermi surfaces are to be studied in detail, an automated Fourier analysis method will probably be essential.

[32] F. R. Fickett, A. F. Clark, and R. L. Powell, Bull. Am. Phys. Soc. 14, 306 (1969).

ACKNOWLEDGMENTS

I would like to thank David Shoenberg for valuable suggestions and for making available before publication the copper Fermi-surface radii as calculated by his student, M. Halse. For useful discussions, I thank, among others, Darrell J. Gillespie and Alexander C. Ehrlich. For continued interest and encouragement, I am grateful to Albert I. Schindler.